Colloid and Polymer Science (2019) 297:903–915
https://doi.org/10.1007/s00396-019-04514-5

ORIGINAL CONTRIBUTION

Effect of nano-SiO_2 and surfactants on the oil-water interfacial properties

Ping Jiang[1] · Lei Zhang[1] · Dengyu Tang[1] · Longjie Li[1] · Jijiang Ge[1] · Guicai Zhang[1] · Haihua Pei[1]

Received: 1 January 2019 / Revised: 26 March 2019 / Accepted: 23 April 2019 / Published online: 15 May 2019

Abstract

This study aimed to clarify the effects of different types of nano-SiO_2 and surfactants on the oil-water IFT and IFR. These interfacial properties were demonstrated to be influenced by the interaction between the surfactant, the nano-SiO_2 and the oil component. The interaction between nano-SiO_2 and oil components and their adsorption at the crude oil-water interface were closely related to the pH values, which, on one hand, determined the amount of charge and the amount of hydroxyl groups on the surface of SiO_2, and on the other hand affected the chargeability of some polar components in the crude oil. Surfactants were observed to compete with other components at the oil-water interface for absorption. When the surfactant concentration was high, the surfactant could replace the colloid and asphaltene at the oil-water interface, and the adsorption of SiO_2 and crude oil components at the oil-water interface was inhibited, which resulted in a relatively low interfacial modulus. The electrostatic interaction between nano-SiO_2 and cationic surfactant and that between nano-SiO_2 and protonated nonionic surfactant could contribute to the formation of composite films at the interface, and thus higher interfacial dilatational modulus, whereas the mutual electrostatic repulsion between nano-SiO_2 and the anionic surfactant would promote one of the two to move towards the interface. Therefore, it could be inferred that different oil-water systems with different interfacial properties could be constructed by adjusting the pH value of the nano-SiO_2 solution, the surfactant type, the molar ratio of the surfactant to the nano-SiO_2, and the oil phase composition.

Keywords Interfacial tension · Surfactant · Crude oil · Dilational rheology · Nanoparticles

Introduction

Emulsifier is commonly used to prepare stable emulsion, due to its capacity of interfacial energy reduction [1]. Moreover, it is also expected to prevent the formation of droplets from coalescence. Therefore, there should be certain kinds of films or barriers forming at the liquid-liquid interface, which are usually single molecule, electrostatic, sterically hindered or liquid crystal. In general, four types of materials can be used as the emulsifier or stabilizer for emulsions, including the ordinary ionic material, colloidal solid particle, polymer, and surfactant.

Surfactants can reduce the pressure difference between the inner and outer curved interfaces of the droplets by decreasing the interfacial tension (IFT), thereby lowering the shear force required for droplet damage [2–5]. Moreover, surfactants can prevent coalescence in emulsification through generating an IFT gradient between two approaching droplets, which can result in a reaction force, contributing to the so-called Gibbs-Marangoni effect. Specifically, the IFT gradient and the Marangoni effect depend on the interfacial dilatational modulus. As for other types of emulsifiers or stabilizers, they vary greatly in their effects and forms of action. Adsorbed ionic materials hardly affect the IFT, and thus have little effect on the emulsification. However, they can enhance the stability of the emulsion system, as the added ions can introduce electrostatic repulsion between adjacent droplets, or contribute to the directional alignment of solvent molecules at the interface, or change some parameters (such as dielectric constant, density, and viscosity) to produce a solvation-based stabilizing effect. Colloidal solid particles can enhance the emulsion stability via forming physical barriers between droplets, such as the particle-stabilized Pickering emulsion. Polymers can stabilize the emulsion mainly through space and electrostatic effects, or changing the interface viscoelasticity and bulk viscosity.

✉ Ping Jiang
jiangping@upc.edu.cn

[1] School of Petroleum Engineering, China University of Petroleum (East China), Qingdao 266580, China

Therefore, in addition to the IFT, the new interfacial dilatational modulus generated during the stirring process is also very important for the emulsion preparation and stability, because the emulsification process is typically featured by the gradual droplet breaking and area fluctuation, and the area fluctuation can be significantly constrained by the interfacial dilatational modulus [6]. It has been demonstrated that a larger interfacial dilatational modulus requires longer stirring time for emulsification, whereas a smaller one requires shorter time, which is favorable for the formation of small droplets [7]. The mechanism of solid particle-stabilized Pickering emulsion has been extensively studied, which is argued to be different from that of surfactant-stabilized emulsion [8, 9]. The stability of Pickering emulsion is achieved by steric hindrance and change of interfacial rheology, rather than through reduction of IFT. However, as for the emulsion systems where the surfactant and particles are co-stabilized, the type and stability of the emulsion depend on the interaction between the two, which manifests in either synergy or competition. Synergy refers to their common efforts to change the particle surface wettability due to the absorption of surfactants on the particle surface, which further influences the emulsion type and stability. Meanwhile, competition refers to the competitive absorption between those unabsorbed surfactants and particles on the oil-water interface, the relative concentration change of which also influences the emulsion type and stability [10].

Synergy

Schulman and Leja [11] pinpointed that the introduction of surfactants into emulsion could change the particle contact angles, which would in turn change the emulsion type, in their research on properties of barium sulfate particle-stabilized emulsions. Tsugita et al. [12] found that the combination of Na-montmorillonite and polar organic compounds, which stabilized the emulsion, could contribute to the formation of water-insoluble compounds, which played a significant role in stabilizing the emulsion droplets by being absorbed on the droplet surface and thus forming a film. Tambe and Sharma [13] proposed the wettability change of $CaCO_3$ particle-stabilized emulsion from the o/w type to the w/o type, as the stearic acid concentration in the oil phase increased, and this was attributed to the absorption of stearic acid molecules on the surface of $CaCO_3$ particles. Binks et al. [14] and Binks and Rodrigues [15] argued that the contact angle reached its maximum when the flocculation in the particle dispersion system peaked, in their research on the stability of the emulsion prepared by the cationic surfactant CTAB/SiO_2 particles and the anionic surfactant SDS/Al_2O_3 coated SiO_2 particles. Correspondingly, the emulsion in this case had the best delamination and aggregation stability, and this was because of the formation of complete adsorption units by surfactants on the particle surface, which corresponded to the strongest particle hydrophobicity and thus the o/w type wettability. Whitby et al. [16] prepared a series of emulsions by combining laponite particles with oil-soluble surfactants, and they identified the synergy between laponite particles and octadecylamine molecules in stabilizing emulsions. This was ascribed to the migration of some octadecylamine molecules from the oil phase to the oil-water interface and their subsequent adsorption on the laponite particle surfaces, which further promoted the particle adsorption on the oil-water interface. Meanwhile, the simultaneously changed surfactant type and concentration were demonstrated to be able to result in the double inversion of the Pickering emulsion [17–22].

Synergy was also reported between nonionic surfactants and particles in co-stabilizing the emulsion. Midmore [23] prepared their emulsions co-stabilized by different types of polyoxyethylene type nonionic surfactants and SiO_2 particles, and found that the addition of surfactants could lead to the formation of flocs with relatively long PEO segments and thus relatively high structural strength, which contributed to the relatively high emulsion stability. Based on their research on the SiO_2-particle and PEO-PPO-PEO block copolymer co-stabilized emulsion system, Gosa and Uricano [24] clarified the effects of the block copolymer molecular weight, the hydrophilic-lipophilic balance (PEO/PPO ratio), and temperature on the interaction between the particles and the block copolymer. Li et al. [25] and Wang et al. [26] prepared their emulsions co-stabilized by polyoxyethylene alkyl ether nonionic surfactant (Brij30 and Brij35) and laponite particles, and found the phenomenon that Brij could be absorbed on the surface of laponite particles, and a relatively low Brij concentration was more favored for the synergy between it and laponite particles in enhancing the emulsion stability.

Competition

When the surfactant is mixed with particles to stabilize the emulsion, the two will compete for adsorption at the oil-water interface. Legrand et al. [27] proposed that flocculation and coalescence would occur when some hydrophobic SiO_2 particles were added in the oil emulsion stabilized by the cationic surfactant. Similar phenomenon was reported by Binks et al. [14], when they added hydrophilic SiO_2 particles in a polyoxyethylene surfactant-stabilized emulsion, which was attributed to the competitive adsorption of surfactants and particles at the oil-water interface. Thijssen et al. [28] added Rhodamine B (fluorescent agent), instead of the surfactant, in the polymethyl methacrylate (PMMA) pellet dispersion system for emulsion preparation, and they observed in the fluorescence confocal microscope that Rhodamine B was not only adsorbed on the surface of the particles to modify the particles, but also adsorbed on the surface of the emulsion droplets. Therefore, it could be inferred that the surfactant and particles competed for adsorption at the oil-water interface in

the emulsion preparation process. Weichold et al. [29] pinpointed the adsorption of dodecylbenzenesulfonic acid on both the particle surfaces and the oil-water interface. Pichot et al. [30] studied the competitive adsorption of particles and surfactants at different surfactant concentrations in the emulsions stabilized by the surfactant Tween60, sodium caseinate and lecithin. Mackie et al. [31, 32] and Wilde et al. [33] systematically analyzed the competitive adsorption of proteins and (nonionic and ionic) surfactants at the interface, and proposed a mechanism for the replacement of proteins by surfactants. In the case that surfactants and particles competed for adsorption at the oil-water interface, the resulting emulsion could even be a surfactant-stabilized emulsion, if the surfactant dominated [21, 34].

It could be seen from the above analysis that the interaction of surfactants and nanoparticles played a key role in the preparation and stability of the emulsion. Correspondingly, three types of typical surfactants were selected to analyze the effect of their compounding with different types of nano-SiO_2 on the oil-water IFT and viscoelasticity. Two important parameters reflecting the interfacial properties were correlated to clarify the competition or synergy between nanoparticles and surfactants. The results showed that different oil-water two-phase systems with different interfacial properties could be constructed by adjusting the pH value of the nano-SiO_2 solution, the surfactant type, the molar ratio of the surfactant to the nano-SiO_2, and the oil phase component.

Experimental

Materials

The water was produced by a Millipore (Elix plus Milli-Q) purifier system, with a conductivity of 18.2 MΩ/cm. The simulated oil was composed of 20 wt% crude oil from Zhuang1-P84 Oilfield, China, and 80 wt% toluene. Three types of surfactants with purities higher than 99% were purchased from Sinopharm (China), which were respectively hexadecyltrimethylammonium Bromide (CTAB), sodium dodecyl sulfate (SDS), and polyethylene glycol tert-octylphenyl ether (TX100).

Two types of nano-SiO_2 were used in the experiments, with the same primary diameter of 12 nm. One was N20 fumed silica nanoparticles (Wacker, German), and the other was Ludox HS30 colloidal silica (Grace, USA).

Methods

IFT measurements

The oil-water IFT (γ) was measured by drop shape tensiometry as a function of time. The classical method was to fit the theoretical profile of an axis-symmetric drop predicted by the Bashforth-Adams equation to measured profiles [35, 36].

A Germany-based KRüSS-manufactured DSA-100 instrument was used to measure the IFT of pendant drops attached to a small stainless steel capillary, with the error less than 0.1 mN/m. This instrument could work well under imposed interfacial area conditions. Images of the drop profiles were recorded over time, while the droplet area was continuously monitored and controlled by means of a precision syringe pump. All measurements were performed at the temperature of 20 °C.

Dilatational rheology measurements

The interfacial dilatational viscoelasticity (or complex interfacial dilatational modulus) was measured by the oscillating drop method using the DSA-100 instrument. The interfacial dilatational rheology could reflect the interfacial deformation and the two-dimensional functional relationship between the deformation velocity and the tension. The interfacial dilatational modulus, ε, was defined as the ratio of the surface pressure (π) to the area change (ΔA) [37]:

$$\varepsilon = \frac{d\pi}{d\ln A} \approx -A\frac{\Delta\pi}{\Delta A}$$

The interfacial dilatational modulus ε is a complex number related to the frequency of interfacial expansion.

$$\varepsilon = |\varepsilon| exp(i\omega t) = \varepsilon_r + i\varepsilon_i = \varepsilon_d + i\omega\eta_d$$

where ω is the moving frequency of the slipper; ε_d is the interfacial dilatational modulus, or storage modulus; η_d is the interfacial dilatational viscosity; and $\omega\eta_d$ is the viscous modulus, which indicates the dissipated energy in various relaxation processes of the interfacial molecules when the interface area is changed.

Dynamic light scattering

Light scattering measurements were performed using a Brookhaven 90Plus PALS in order to evaluate the presence of silica particles in surfactant solutions that had been equilibrated with particle dispersions.

Results and discussion

Nano-SiO_2 evaluation

Two different particle size distributions were observed after the dispersion of fumed silica nanoparticles and colloidal silica into water. First of all, as shown in Fig. 1, the colloidal silica system after dispersion was featured by smaller particle size and narrower particle size distribution range, and

coalescence occurred after the dispersion of fumed silica nanoparticles in water.

Secondly, the pH of the systems with fumed silica nanoparticles and colloidal silica would also change differently with different SiO_2 concentrations, as shown in Table 1. For fumed silica nanoparticles, the pH of their solution gradually decreased as the concentration increased, finally presenting weak acidity. However, the pH of the solution of colloidal silica increased as the concentration increased, finally presenting weak basicity.

Zeta potential of both particles were measured at different pH values, (Fig. 2), which shared similarity. Isoelectric points (IEPs) were located at pH values of 2–3.

Figure 3 displays changes of particle sizes of two particles at different pH values. The particle size of colloidal silica hardly changed with pH. In contrast, the particle size of fumed silica dropped at high pH values, and this could be attributed to the partially broken Si–O–Si bonds between particles under the action of NaOH, which reduced the particle size of the agglomerate.

Table 1 pH of fumed silica nanoparticles and colloidal silica

Concentration of SiO_2/wt%		0	0.1	0.2	0.3
pH	Fumed silica nanoparticles	6.1	5.6	5.4	5.0
	Colloidal silica		9.0	9.3	9.5

IFT between oil and nano-SiO_2 solution

Figure 4 shows the effect of nanoparticles on the oil-water IFT, which decreased slowly with time, mainly due to the presence of interfacial active components in the simulated oil and their adsorption on the interface. However, it should be noted here that both the decreasing rate and magnitude were relatively low in this case. Then, the addition of different nanoparticles was observed to be associated with distinct oil-water IFT changes. Specifically, the addition of fumed silica nanoparticles led to insignificant IFT variation, whereas that of colloidal silica dramatically lowered the IFT from 25 to 18 mN/m. This was attributed to the formation of materials with stronger interfacial

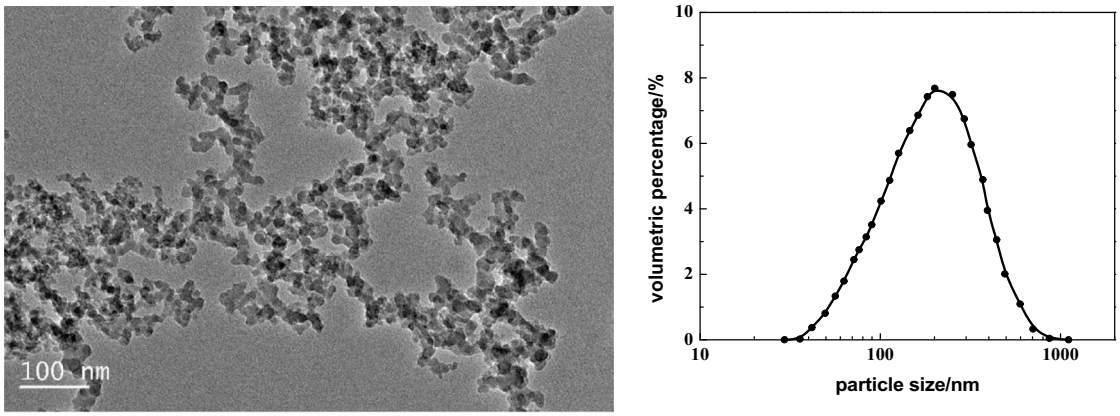

(a) Particle size and its distribution of fumed silica nanoparticles in water

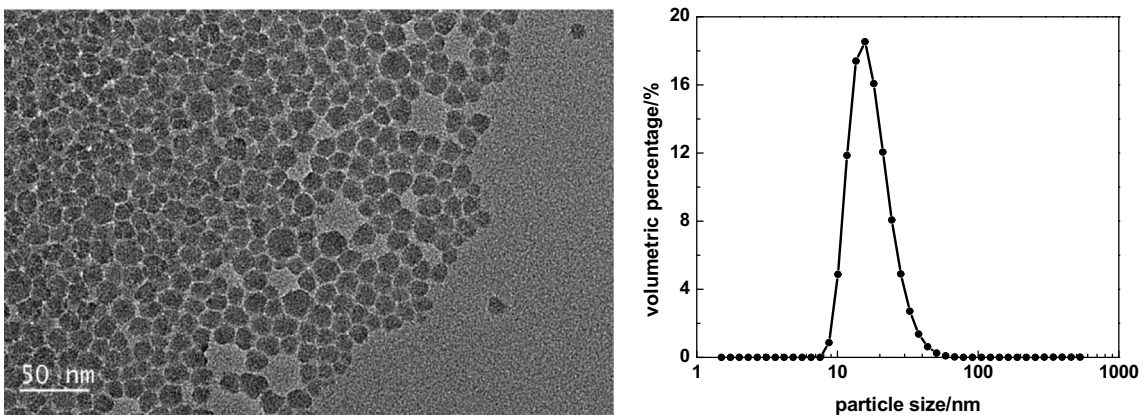

(b) Particle size and its distribution of colloidal silica in water

Fig. 1 Particle size distribution of fumed silica nanoparticles and colloidal silica

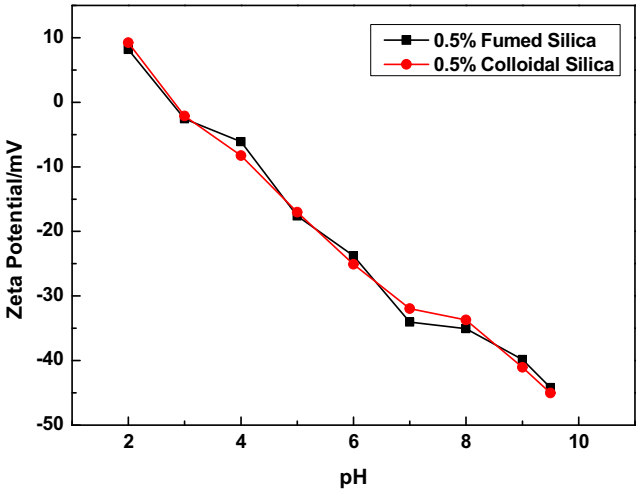

Fig. 2 Relationship between zeta potentials of two particles and pH

activity by the reaction between the weakly alkaline collosol system and the acidic materials in the crude oil.

As shown in Fig. 5, the IFT was significantly decreased due to the addition of colloidal silica, whereas the addition of fumed silica nanoparticles contributed to small IFT variation. Therefore, it could be inferred that the exclusive addition of fumed silica nanoparticles would not influence IFT much, which might be due to the difficulty that particles were faced with in being absorbed on the oil-water interface. In this context, increasing sol concentration could also increase the amount of alkaline substance that reacted with the crude oil, thereby reducing IFT as sol concentration increased.

Influence of SiO_2 on IFT in systems with different surfactants

The combination of suitable surfactants and nanomaterials can effectively reduce the concentration of emulsifier as required by the emulsion preparation, and greatly improve the stability of the emulsion, both of which could be attributed to the good

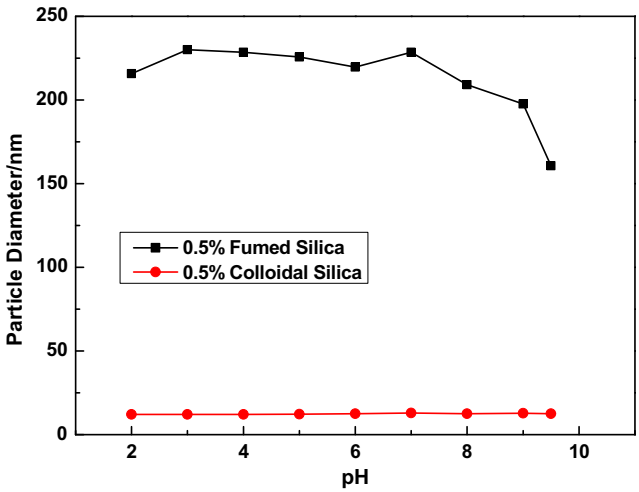

Fig. 3 Relationship between particle sizes and pH 3.2 IFT measurement

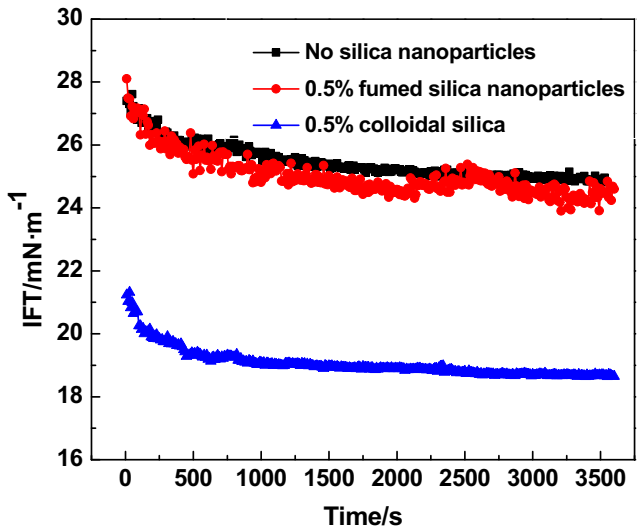

Fig. 4 IFT curves corresponding to the systems with no SiO_2, addition of 0.5% fumed silica nanoparticles, and addition of 0.5% colloidal silica

synergy between surfactants and nanomaterials. Therefore, this study explored the influence of combinations of different surfactants and nanomaterials on the oil-water IFT, in order to clarify the synergistic relationship between different surfactants and nanomaterials.

Figure 6 (lines 4, 7, 9) shows the oil-water IFT corresponding to the combination of 0.005% cationic surfactant CTAB and nano-SiO_2. It could be observed that the addition of surfactants could largely reduce the IFT. Moreover, the compounding between CTAB and fumed silica nanoparticles resulted in similar IFT at first and then slightly increased IFT, whereas the compounding between CTAB and colloidal silica enhanced the IFT. Overall, this kind of difference was thought to be due to the different adsorption between cationic surfactants and negatively charged nano-SiO_2. Specifically, the system with fumed silica

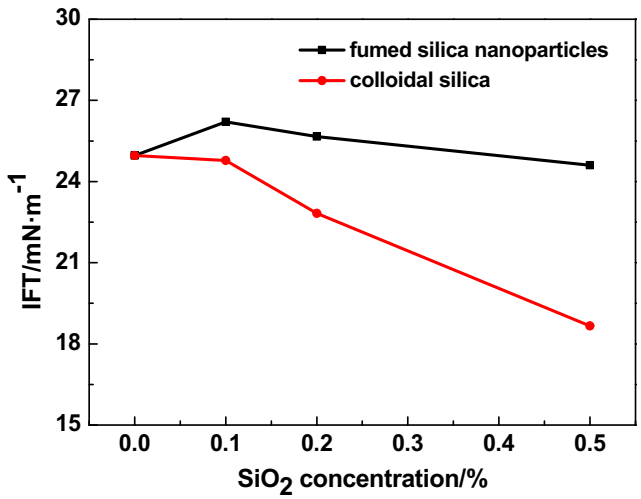

Fig. 5 Equilibrium IFT curves corresponding to systems with fumed silica nanoparticles and colloidal silica

nanoparticles was overall acidic (pH = ~ 5.0), and the nitrogen-containing components in the crude oil were positively charged [38]. The insignificantly decomposed acidic components and the increasing hydroxyl groups on the SiO_2 surface reacted to each other, forming composite structures at the interface by electrostatic and hydrogen bonding. Thereby, the surfactant-adsorbed particles were moved to the oil-water interface, which resulted in a similar IFT to that in the surfactant-simulated oil system. Contrastingly, the system with colloidal silica was overall alkaline (pH = ~ 9.5). The overall negatively charged polar components in the crude oil and the strongly negatively charged SiO_2 were mutually exclusive, which failed to result in coalescence at the oil-water interface. Thus, the adsorption of surfactants and particles reduced the effective concentration of the bulk phase and that of free phase surfactants at the interface, which led to the higher IFT

Figure 6 (lines 2, 6, and 8) shows the oil-water IFT corresponding to the combination of 0.005% anionic surfactant SDS and nano-SiO_2. It could be seen that the introduction of fumed silica nanoparticles could reduce the dynamic IFT compared to the solution with exclusive SDS, whereas that of colloidal silica greatly enhanced the dynamic IFT. It should be noted here that the surfactant concentration was very low in this experiment. The reaction between fumed silica nanoparticles surfaces and materials in the crude oil contributed to the movement of some solid materials to the interface, which occupied the space where SDS should be absorbed, thereby increasing the IFT. However, the alkaline property of the colloidal silica system made it difficult to form hydrogen bonds between particles and components in the simulated oil.

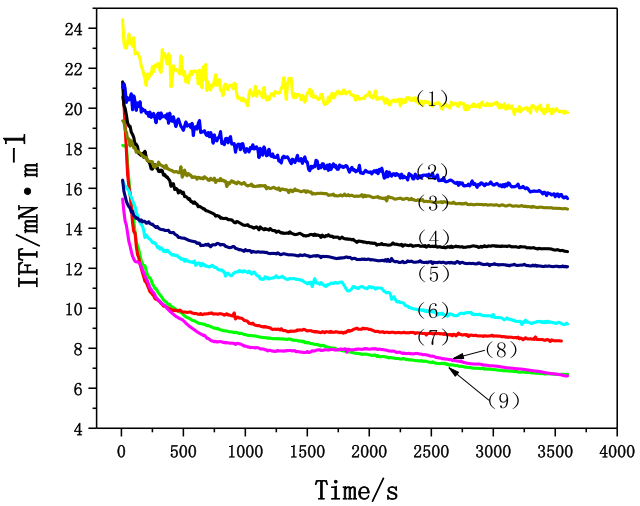

Fig. 6 Dynamic IFT of the oil and SiO_2 system with surfactants and nanoparticles. (1) 0.005% TX100 + 0.5% fumed silica nanoparticles, (2) 0.005% SDS + 0.5% fumed silica nanoparticles,(3) 0.005% TX100, (4) 0.005% CTAB+ 0.5% colloidal silica, (5) 0.005% TX100 + 0.5% colloidal silica, (6) 0.005% SDS, (7) 0.005% CTAB+ 0.5% fumed silica nanoparticles, (8) 0.005% SDS + 0.5% colloidal silica, and (9) 0.005% CTAB

Moreover, the electrostatic repulsion between SDS and colloidal silica promoted the adsorption of SDS in the solution at the oil-water interface. Furthermore, the alkaline colloidal silica system could react with the acidic components in the simulated oil, forming interface-active substances, thereby accelerating the IFT reduction

Figure 6 (line 1, 3, and 5) shows the oil-water IFT corresponding to the combination of 0.005% nonionic surfactant TX100 and nano-SiO_2. It could be seen that the introduction of fumed silica nanoparticles could enhance the dynamic IFT compared to the solution with exclusive TX100, whereas that of colloidal silica greatly lowered the dynamic IFT. Specifically, the alkaline colloidal silica could react with the acidic components in the simulated oil, forming interface-active substances, thereby decreasing the IFT together with TX-100. Though the weakly acidic fumed silica nanoparticles could contribute to the adsorption between TX-100 and fumed silica nanoparticles by positively charging protons of TX-100, the absorption between nano-SiO_2 and CTAB was demonstrated to be stronger. Therefore, nano-SiO_2 was more adsorbed at the oil-water interface due to the hydrogen bonding with the crude oil components, which reduced the adsorption amount of TX-100 at the interface, thereby resulting in high IFT

As shown in Fig. 7, IFT gradually decreased as the surfactant concentrations increased, and the influence of nanoparticles on the equilibrium IFT was similar to that on the dynamic IFT.

Interfacial dilatational rheology with oscillating drop measurements

Although not the exclusive factor, the dilatational rheology plays an important role in affecting the emulsion stability. Due to the difficulty in measuring the interfacial dilatational viscoelasticity in the early experiments, more attention was paid to the relationship between interfacial shear viscosity and interfacial shear modulus and emulsion and foam stability. With the progress of theory and instrumental measurement, it has been found that the interfacial dilatational viscosity is generally several orders of magnitude larger than the interfacial shear viscosity, and the dilatational viscosity accounts for the majority of the overall interfacial viscosity. Therefore, it has been gradually realized that the stability of emulsion and foam should be more controlled by the interfacial dilatational viscoelasticity, whereas the exclusive use of shear rheological data should be insufficient to predict the stability of droplets. Correspondingly, it is recommended to comprehensively combine the dilatational and shear rheological data for prediction [39, 40]. In the past decade, a lot of work has been conducted on the interfacial dilatational viscoelasticity [6, 41–44].

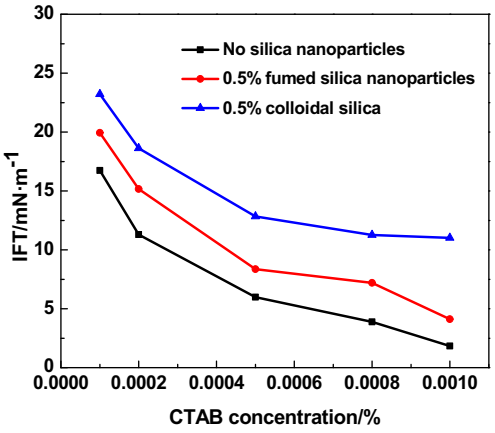

(a)

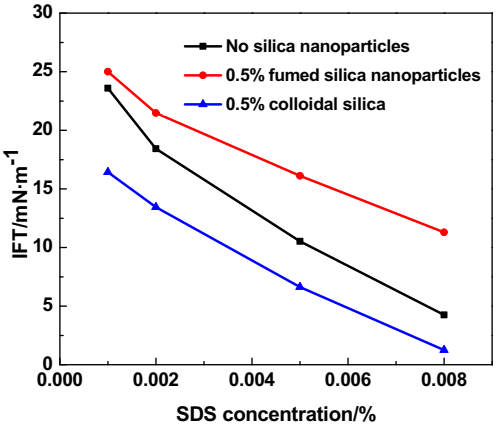

(b)

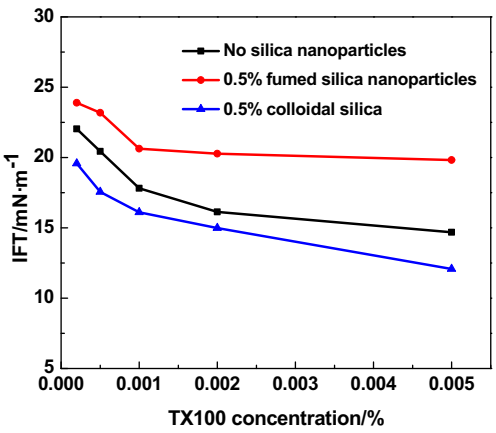

(c)

Fig. 7 Equilibrium IFT with different surfactant concentrations

Interfacial dilatational rheology between oil and nano-SiO_2 solution

Figure 8 shows the variation of the interfacial modulus with frequency at amplitude of 0.2 μL. It could be seen that the interfacial film was mainly elastic when the interfacial elastic modulus was greater than the viscous

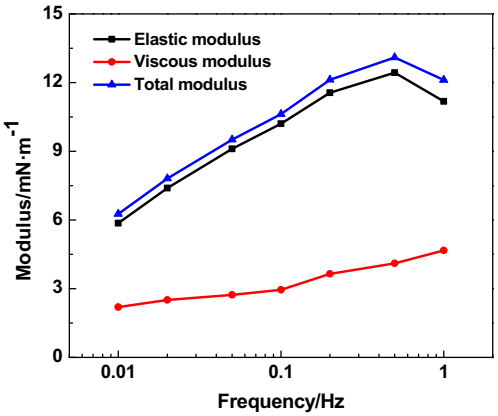

Fig. 8 Variation of the interfacial modulus with frequency when the amplitude was 0.2 μL

modulus. Meanwhile, the dilatational modulus increased with the increase of the angular frequency. For the interfacial dilatational rheology, there was movement of molecules from the interface to the bulk phase or from the bulk phase to the interface when the interface was compressed or expanded, thereby maintaining molecular concentration equilibrium at the interface [6, 45, 46]. At lower frequencies, the molecular concentration at the interface had sufficient time to reach equilibrium during each cycle of expansion and compression, so that IFT only changed slightly and the viscoelastic modulus was relatively small. Conversely, at higher frequencies, the exchange of molecules between the interface and the bulk phase was much slower than the frequency disturbance, in which condition the interfacial molecular layer was like an insoluble monolayer, resulting in a higher viscoelasticity.

Figure 9 shows the variation of the interfacial modulus with time. It could be seen that all the total modulus, elastic modulus, and viscous modulus increased with time, which could be attributed to the migration of polar components in the simulated oil (colloidal, asphaltene) to

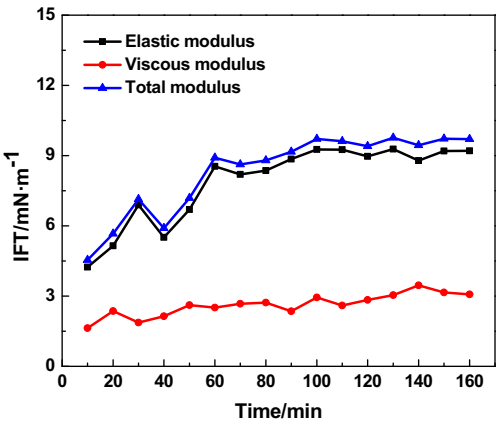

Fig. 9 Interfacial modulus of the system without SiO_2

the oil-water interface, thereby increasing the interfacial viscoelasticity. At the same time, the elastic modulus of the system was always greater than the viscous modulus, indicating that the oil-water interface should be mainly elastic.

Figure 10 shows the change of interfacial modulus with time after adding 0.5% colloidal silica. Unlike the simple oil-water interface film, the modulus in this case did not increase significantly with time, and this was mainly ascribed to the formation of interface-active substance by the oil-water system in an alkaline environment, which could reduce the interfacial modulus and thus offset certain influence of the crude oil components.

Figure 11 shows the change of interfacial modulus with time after adding 0.5% fumed silica nanoparticles. The dramatically increased interfacial modulus, especially the elastic modulus, was mainly attributed to the formation of composite structures at the interface by reaction between weakly acidic fumed silica nanoparticles and crude oil components through electrostatic interaction and hydrogen bonding, which could increase the interfacial modulus. Moreover, the adsorption of the nanoparticles at the interface suppressed the adsorption of some active substances, resulting in a gradually lowered viscous modulus.

Figure 12 shows the variation of the elastic modulus, viscous modulus, and total modulus with the SiO_2 concentration. It was observed that colloidal silica had a relatively small influence on the interfacial modulus, reflected in the slowly lowered interfacial modulus with the increase of the SiO_2 concentration. This could be attributed to the reaction between the alkaline materials in the collosol and the petroleum acids in the simulated oil, resulting in the formation of surface-active substance that could lower the interfacial modulus. Contrastingly, fumed silica nanoparticles could enhance the elastic modulus and total modulus of the oil-water interface by hydrogen bonding and electrostatic adsorption with the crude oil components.

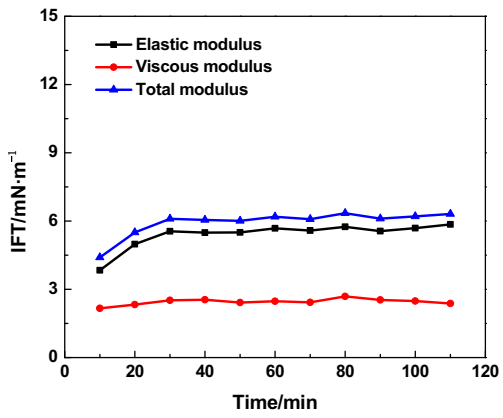

Fig. 10 Interfacial modulus of the system with 0.5% colloidal silica

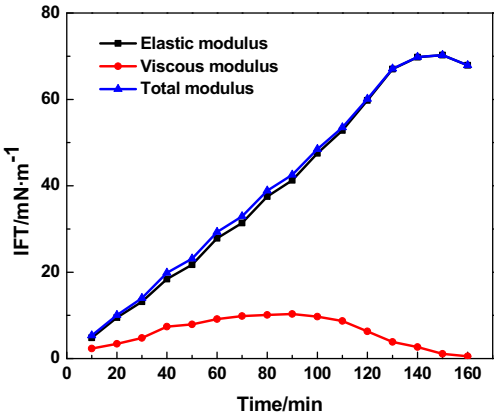

Fig. 11 Interfacial modulus of the system with 0.5% nano-SiO_2 particle

Influence of SiO_2 compounded with different types of surfactants on interfacial dilatational rheology

Figure 13 shows the effect of different concentrations of CTAB on the interfacial modulus. It could be seen that the compounding between CTAB and fumed silica nanoparticles had a greater influence on the interfacial modulus than the compounding between CTAB and colloidal silica. Specifically, fumed silica nanoparticles could be absorbed on the interface through hydrogen bonding and electrostatic interaction. When the surfactant concentration was low, the interface layer mainly consisted of nanoparticles and a small amount of surfactant molecules. And in this case, the surfactant molecules could be combined with SiO_2 through electrostatic interaction, thereby promoting an increase in interfacial dilatational modulus. As the surfactant concentration increased, more and more surfactant molecules moved to the interface, and participated in the formation of the interfacial network structure through electrostatic and hydrophobic interactions, while promoting the interfacial dilatational modulus to further increase. However, it was noticed that, the combination between surfactants and SiO_2 would peak somehow when the concentration of CTAB exceeded a certain value, which corresponded to the maximum interfacial dilatational modulus. If the concentration of CTAB was further enhanced, then strong electrostatic interaction between the surfactant and SiO_2 would occur, which could destroy the network structure. Moreover, more and more surfactants in the bulk phase were bound to SiO2, which could result in the continuous desorption of SiO_2 from the interface layer, thereby destroying the network structure at the interface and thus reducing the interfacial dilatational modulus. As for the colloidal silica, it was observed to only have a relatively large influence on the interfacial viscoelasticity when the concentration of CTAB was relatively large. This was due to the role of higher CTAB concentration in promoting the combination of surfactants and SiO_2 as well as the

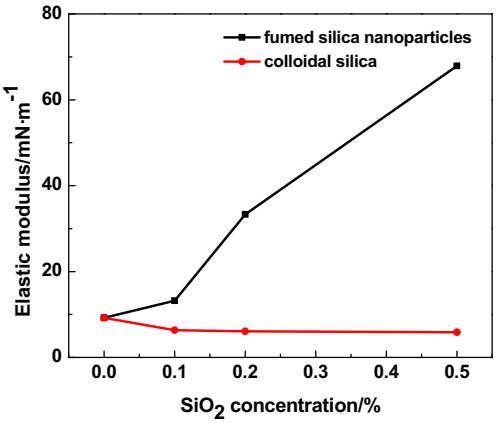

(a)

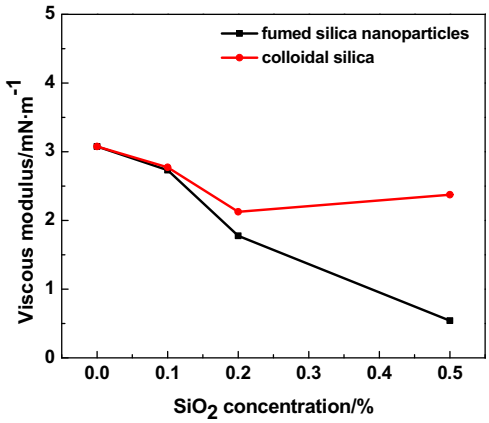

(b)

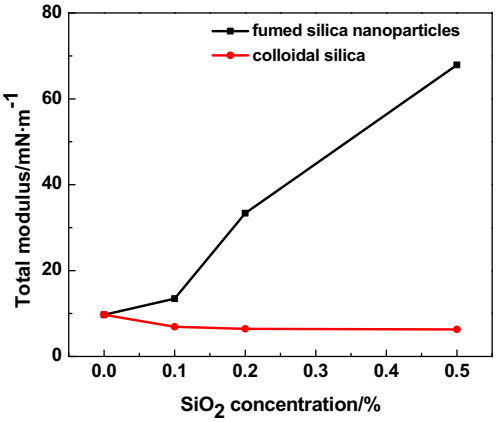

(c)

Fig. 12 Variation of the modulus with nano-SiO_2 concentrations

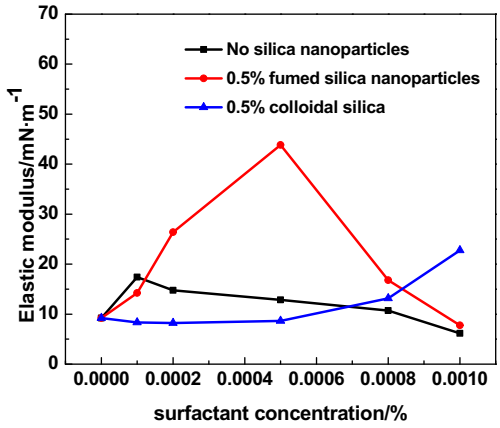

(a)

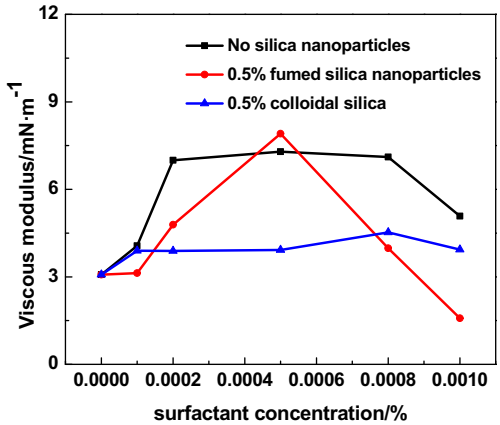

(b)

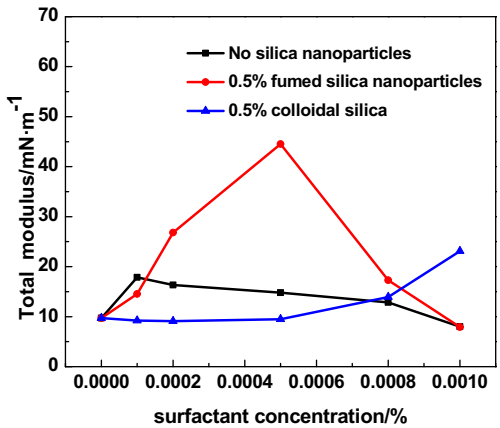

(c)

Fig. 13 Variation of the modulus in the systems with CTAB concentrations

migration of surfactants to the interface, which resulted in the movement of SiO_2 to the oil-water interface and subsequent formation of composite adsorption film that increased the interfacial viscosity of the system.

As shown in Fig. 14, the effect of different concentrations of SDS on the interfacial modulus was similar to that of CTAB. And again the compounding between SDS and fumed silica nanoparticles had a greater influence on the interfacial modulus than the compounding between SDS and colloidal silica. When the SDS concentration was low, both the electrostatic repulsion between SDS and fumed silica nanoparticles as well as the combination of fumed silica nanoparticles and crude oil components enhanced the elastic modulus of the oil-water interface. However, when the SDS concentration

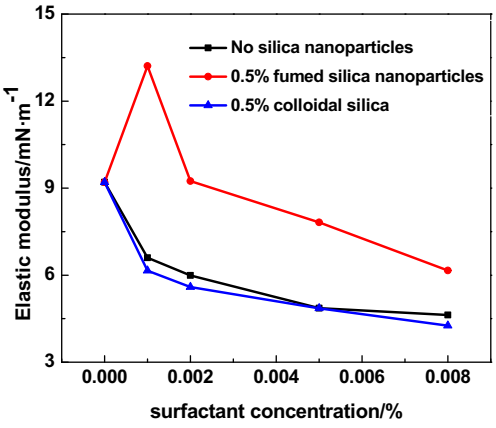

(a)

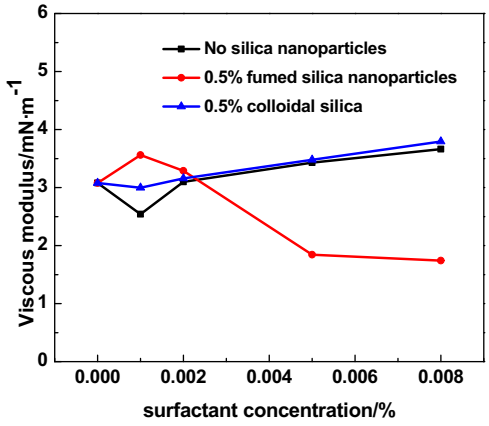

(b)

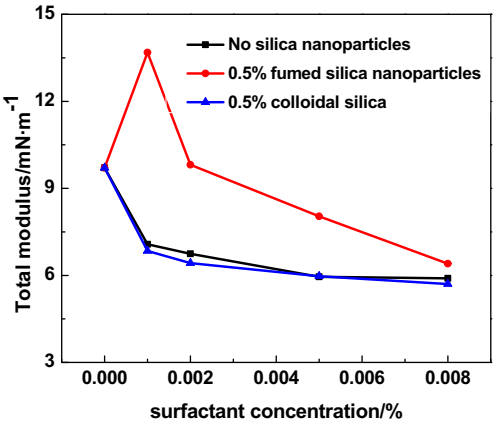

(c)

Fig. 14 Variation of the modulus in the systems with SDS concentrations

continued to increase, SDS competed with fumed silica nanoparticles for adsorption, which would result in the replacement of fumed silica nanoparticles and thus lowered interfacial modulus. As for the colloidal silica, it did not combine with surfactants nor with crude oil components, which resulted in a similar interfacial modulus curve to that of the SiO_2-free system. The decrease of interfacial elasticity and the increase of interfacial viscosity were mainly due to the increase of surfactant concentration and thus the surfactant absorption at the interface.

Figure 15 shows the effect of different concentrations of TX-100 on the interfacial modulus. It could be seen that fumed silica nanoparticles could more significantly enhance the viscoelasticity of the oil-water interface, in the condition with a higher surfactant concentration. It was also noticed that

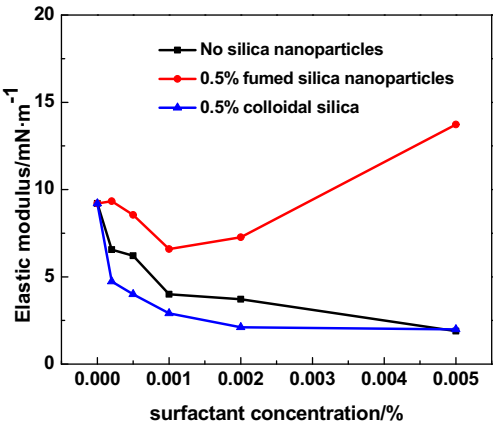

(a)

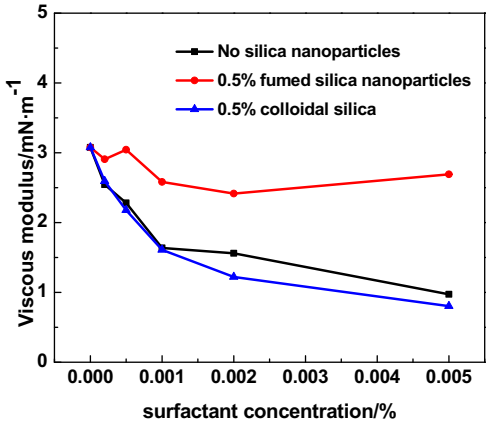

(b)

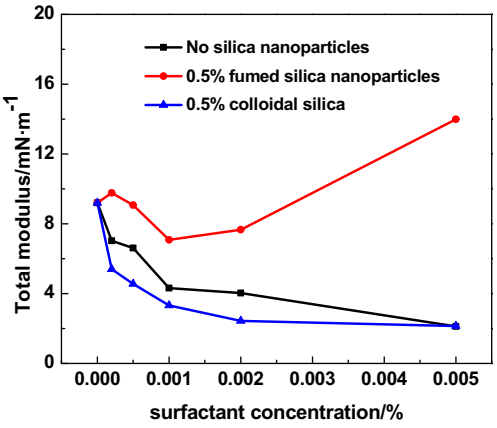

(c)

Fig. 15 Variation of the modulus in the systems with TX100 concentrations

the threshold of the concentration of TX-100 required for interfacial viscoelasticity enhancement was higher than those of CTAB and SDS. This could be attributed to the dominant protonation effect in the TX-100 that contributed to the nano-SiO_2 particle adsorption, which was weaker than the adsorptions in the nano-SiO_2 systems with CTAB. Moreover, TX-100 had an overall larger molecular weight, which contributed to the higher surfactant concentration at the adsorption layer of the composite interface.

It was concluded based on the effect of different surfactants and different types of nano-SiO_2 on the interfacial dilatational modulus that fumed silica nanoparticles played the most significant role in determining the interfacial viscoelasticity, and pH values dominantly influenced the adsorption of fumed silica nanoparticles on the interface. Accordingly, pH values were varied in different kinds of nano-SiO_2 systems, and the variation of the interfacial dilatational modulus with time was recorded.

Figure 16 displays changes of particle sizes after surfactants with different mass fractions were compounded with nanoparticles. Specifically, particle sizes of fumed silica nanoparticles and colloidal silica nanoparticles grew as surfactant concentration increased in the CTAB system, which could be attributed to absorption on their particle surfaces due to electrostatic action. In contrast, particle sizes were independent of surfactant concentration in the SDS system, as SDS and both particles were electrically mutually exclusive, which meant no absorption. The particle size of fumed silica nanoparticles rose as the surfactant concentration increased in the TX100 system, whereas that of colloidal silica nanoparticles rarely changed. This could be explained by the fact that TX100 was exclusively absorbed on surfaces low-pH fumed silica nanoparticles, rather than on surfaces of high-pH colloidal silica nanoparticles.

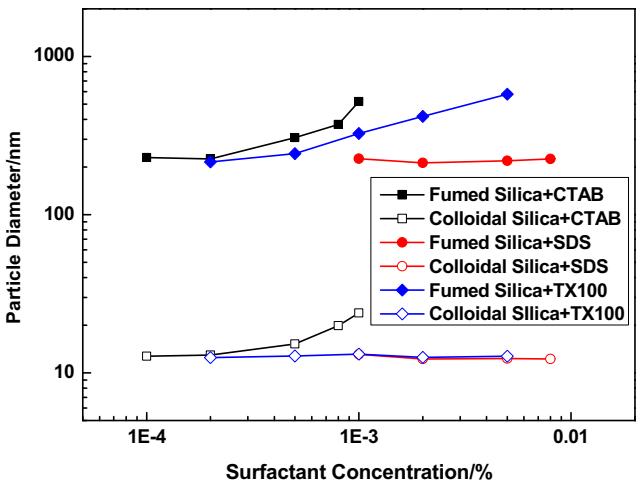

Fig. 16 Relationship between particle sizes and surfactant concentration

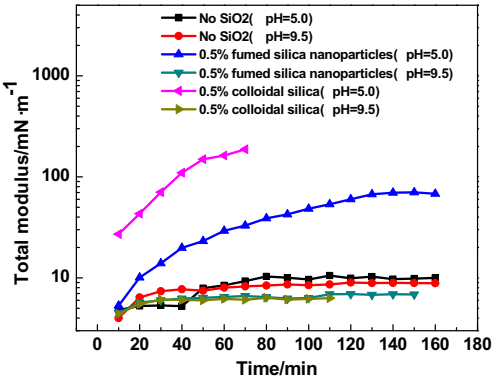

Fig. 17 Effect of nano-SiO_2 on interfacial dilatational modulus at different pH values

It could be seen from Fig. 17 that both fumed silica nanoparticles and colloidal silica nanoparticles could be effectively absorbed on the interface to form insoluble films and thus increase the viscoelasticity of the system, when the pH was smaller than 7. However, when the overall environment was weakly alkaline, the system with fumed silica nanoparticles or colloidal silica had a slightly lower interfacial viscoelasticity than that free of nano-SiO_2, which could be ascribed to the reaction between alkaline substance and petroleum acid and subsequently the formation of surface active substance that could reduce the interfacial dilatational modulus.

Conclusion

The effect of the compounding between different types of surfactants and nano-SiO_2 on the IFT and the interfacial dilatational modulus was determined by three main factors. The first one was the interaction of nano-SiO_2 with crude oil components. It was known that the adsorption of nano-SiO_2 at the interface was closely related to pH, which, on one hand, determined the amount of charge and the amount of hydroxyl groups on the surface of SiO_2, and on the other hand affected the chargeability of some polar components in crude oil. When the pH was high (> 9.5), the generally negatively charged polar components in the crude oil and the strongly negatively charged SiO_2 would be mutually exclusive, which made it difficult for their coalescence at the oil-water interface. When the pH was low (< 5.0), some of the nitrogen-containing components in the crude oil could be positively charged, the acidic components had a low degree of decomposition, and the number of hydroxyl groups on the surface of SiO_2 increased. In this case, SiO_2 could be easily combined with these crude oil components through electrostatic effect and hydrogen bonding, forming composite structures at the interface and thus increasing the interfacial elastic modulus. The second one was the competitive adsorption of surfactants at the oil-water interface. When the surfactant concentration was high, the surfactant could replace the colloid and

asphaltene at the oil-water interface, and the adsorption of SiO_2 at the oil-water interface was inhibited, which resulted in a relatively low interfacial modulus. The third one was the synergy between nano-SiO_2 and surfactants. The electrostatic effect between nano-SiO_2 and cationic surfactant (CTAB) and that between nano-SiO_2 and protonated nonionic surfactant (TX-100) could enhance their adsorption at the interface, which was beneficial to the formation of composite films at the interface, whereas the mutual electrostatic repulsion between nano-SiO_2 and the anionic surfactant (SDS) would promote one of the two to move towards the interface.

Funding information The study is financially supported by the National Natural Science Foundation of China (No. 51474234) and the Fok Ying Tung Education Foundation (No.151049) and the Fundamental Research Funds for the Central Universities (No.19CX02017A).

Compliance with ethical standards

Conflict of interest The authors declare that they have no conflict of interest.

References

1. Pashley RM, Karaman ME (2004) Applied colloid and surface chemistry, 1st. Wiley, New York Chap.5
2. Vincent AN, Gert F (2001) Marangoni flow driven instabilities and marginal regeneration. J Colloid Interface Sci 234:162–167
3. Bibette J (2005) Interface:their role in foam and emulsion behavior. Curr Opin Colloid Interface Sci 5:176–181
4. Klitzing RV, Müller HJ (2002) Film stability control. Curr Opin Colloid Interface Sci 7:42–49
5. Capek I (2004) Degradation of kinetically-satble o/w emulsion. Adv Colloid Interf Sci 107:125–155
6. Langevin D (2000) Interfacial rheology on foam and emulsion properties. Adv Colloid Interface Sci 88:209–222
7. Santini E, Liggieri L, Sacca L, Clausse D, Ravera F (2007) Interfacial rheology of Span 80 adsorbed layers at paraffin oil-water interface and correlation with the corresponding emulsion properties. Colloids Surface A 309:270–279
8. Tambe DE, Sharma MM (1995) Factors controlling the stability of colloid-stabilized emulsions: III. Measurements of the rheological properties of colloid-laden interfaces. J Colloid Interface Sci 171: 456–462
9. Okubo T (1995) Surface tensin of structured colloidal suspensions of polystyrene and silica spheres at the air-water interface. J Colloid Interface Sci 171:55–62
10. Vignati E, Piazza R, Lockhart TP (2003) Pickering emulsions: interfacial tension, colloidal layer morphology, and trapped-particle. Langmuir 19:6650–6656
11. Schulman JH, Leja J (1954) Control of contact angles at the oil-water-splid interfaces. Emulsion stabilized by solid particles ($BaSO_4$)[J]. Trans Faraday Soc 50:598–605
12. Tsugita A, Takemoto S, Mori K, Yoneya T, Otani Y (1983) Studies on O/W emulsions stabilized with insoluble montmorillonite-organic complexes[J]. J Colloid Interface Sci 95:551–560
13. Tambe DE, Sharma MM (1994) The effect of colloidal particles on fluid-fluid interfacial properties and emulsion stability [J]. Adv Colloid Interf Sci 52:1–63
14. Binks BP, Rodrigues JA, Frith WJ (2007) Synergistic interaction in emulsions stabilized by a mixture of silica nanoparticles and cationic surfactant[J]. Langmuir 23:3626–3636
15. Binks BP, Rodrigues JA (2007) Enhanced stabilization of emulsions due to surfactant-induced nanoparticle flocculation[J]. Langmuir 23:7436–7439
16. Whitby CP, Fornasiero D, Ralston J (2008) Effect of oil soluble surfactant in emulsions stabilized by clay particles[J]. J Colloid Interface Sci 323:410–419
17. Binks BP, Rodrigues JA (2007) Double inversion of emulsions by using nanoparticles and a di-chain surface[J]. Angew Chen Int Ed 46:5389–5392
18. Binks BP, Rodrigues JA (2009) Influence of surfactant structure on the double inversion of emulsions in the presence of nanoparticles[J]. Colloid Surf A Physicochem Eng Asp 345:195–201
19. Cui ZG, Yang LL, Cui YZ et al (2009) Effects of surfactant structure on the phase inversion of emulsions stabilized by mixtures of silica nanoparticles and cationic surfaciant[J]. Langmuir
20. Cui ZG, Yang LL, Cui YZ et al (2008) Double phase invension of emulsions stabilized by a mixture of $CaCO_3$ nanoparticles and sodium dodecyl sulphate[J]. Colloid Surf A Physicochem Eng Asp 329:67–74
21. Wang J, Yang F, Li CF, Liu S, Sun D (2008) Double phase inversion of emulsions containing layered double hydroxide particles induced by adsorption of sodium dodecyl sulfate[J]. Langmuir 24:10054–10061
22. Cui ZG, Cui CF, Zhu Y et al (2011) Multiple phase inversion of emulsions stabilized by in situ surface activation of $CaCO_3$ nanoparticles via adsorption of fatty acids[J]. Langmuir 28:314–320
23. Midmore BR (1998) Synergy between silica and polyoxyethylene surfactants in the formation of O/W emulsions[J]. Colloids Surface A Physicochem Eng Asp 145:133–143
24. Gosa KL, Uricanu V (2002) Emulsions stabilized with PEO-PPO-PEO block copolymers and silica[J]. Colloids Surface A Physicochem Eng Asp 197:257–269
25. Li CF, Zhang SY, Wang J et al (2008) Interactions between Brij suffactants and laponite nanoparticles and emulsions stabilized by their mixtures[J]. Acta Chim Sin 66:2313–2320
26. Wang J, Yang F, Tan JJ, Liu G, Xu J, Sun D (2010) Pickering emulsions stabilized by a lipophilic surfactant and hydrophilic platelike particles[J]. Langmuir 26:5397–5404
27. Legrand J, Chamerois M, Placin F, Poirier JE, Bibette J, Leal-Calderon F (2005) Solid colloidal particles inducing coalescence in bitumen-in-water emulsions[J]. Langmuir 21:64–70
28. Thijssen JHJ, Schofield AB, Clegg PS (2011) How do(fluorescent)surfactants affect particle-stabilized emulsions?[J]. Soft Matter 7:7965–7968
29. Tigges B, Dederichs T, Moeller M et al (2010) Interfacial properties of emulsions stabilized with surfactant and nonsurfactant coated boehmite nanoparticles[J]. Langmuir 26:17913–17918
30. Pichot R, Spyropoulos F, Norton IT (2010) O/W emulsions stabilized by both low molecular weight surfactants and colloidal particles: the effect of surfactant type and concentration[J]. J Colloid Interface Sci 352:128–135
31. Mackie AR, Gunning AP, Wilde PJ, Morris VJ (2000) Competitive displacement of β-lactoglobulin from the air/water interface by sodium dodecyl sulfate[J]. Langmuir 16:8176–8181
32. Mackie AR, Gunning AP, Wilde PJ, Morris VJ (2000) Orogenic displacement of protein from the air/water interface[J]. Langmuir 16:2242–2247
33. Wilde P, Mackie A, Husband F, Gunning P, Morris V (2004) Protein and emulsifiers at liquid interfaces[J]. Adv Colloid Interf Sci 108–109:63–71

34. Vashisth C, Whitby CP, Fornasiero D, Ralston J (2010) Interfacial displacement of nanoparticles by surfactant molecules in emulsions[J]. J Colloid Interface Sci 349:537–543
35. Bashforth F, Adams C (1883) An attempt to test the theories of capillary action. Cambridge University Press, Cambridge
36. Liggieri L, Passerone A (1989) An automatic technique for measuring the surface tension of liquid metals. High Temp Technol 7: 82–86
37. Li JB, Kretzschmar G, Miller R, Möhwald H (1999) Viscoelasticity of phospholipid layers at different fluid interfaces. Colloids Surf A 149:491–497
38. Jiang P, Li N, Ge J, Zhang G, Wang Y, Chen L, Zhang L (2014) Efficiency of a sulfobetaine-type surfactant on lowering IFT at crude oil–formation water interface. Colloids Surfaces A 443: 141–148
39. Miller R, Wfistneck R, Krfigel J et al (1996) Dilational and shear rheology of adsorption layers at liquid interfaces. Colloids Surfaces A Physicochem Eng Asp 111:75–118
40. Williams A, Janssen JJM, Prins A (1997) Behavior of droplets in simple shear flow in the presence of a protein emulsifier. Colloids Surfaces A Physicochem Eng Asp 125:189–200
41. Orozco JPP, Beristain CI, Paredes GE et al (2004) Interfacial shear rheology of interacting carbohydrate at the water-oil interface using an adapted conventional rheometer. Carbohydr Polym 57:45–54
42. Ravera F, Ferrari M, Santini E, Liggieri L (2005) Interface of surface process on the dilational visco-elasticity of surfactant solutions. Adv Colloid Interf Sci 117:75–100
43. Ivanov IB, Danov KD, Ananthapadmanabhan KP, Lips A (2005) Interfacial rheology of adsorbed layers with surface reaction: on the origin of the dilatational surface viscosity. Adv Colloid Interf Sci 114-115:61–92
44. Santini E, Liggieri L, Sacca L (2007) Span 80 absorbed layers at paraffin oil-water interface and correlation with the corresponding emulsion properties. Colloid Surface A 309:270–279
45. Monteux C, Fuller GG, Bergeron V (2004) Shear and dilational surface rheology of oppositely charged polyelectrilyte/surfactant microgels adsorbed at the air-water interface. Influence on foam stability. J Phys Chem B 108(42):16473–16482
46. Noskov BA, Akentiev AV, Bilibin AY, Zorin IM, Miller R (2003) Dilational surface viscoelasticity of polymer solutions. Adv Colloid Interf Sci 104(1–3):245–271